Webology, Volume 18, Number 5, 2021
ISSN: 1735-188X
DOI: 10.29121/WEB/V18I5/25

By using HFC Refrigerants in condensations to estimate the Heat transfer coefficients on high Temperature Tube

Pravin P Patil[1], Manish Kumar Lila[2], Yatika Gori[3], Durgeshwar Pratap Singh[4]

[1]Department of Mechanical Engineering,Graphic Era Hill University, Dehradun, Uttarakhand India, 248002
[2]Department of Mechanical Engineering,Graphic Era Deemed to be University, Dehradun, Uttarakhand India, 248002
[3]Department of Mechanical Engineering,Graphic Era Deemed to be University, Dehradun, Uttarakhand India, 248002
[4]Department of Mechanical Engineering,Graphic Era Deemed to be University, Dehradun, Uttarakhand India, 248002

ABSTRACT

Air conditioning units rely heavily on chlorofluorocarbons. These are typically present in hydrocarbon forms. Refrigerators are employed to cool a specific area. There are various kinds of coolants that act to remove heat from one region as well as distribute it to other regions that necessitate it. Certain coolants are found in a variety of equipment, like air conditioning units and refrigeration devices. These generally use nonlinear behaviour in thermodynamics to convert a gaseous to a fluid and vice versa. The actual heat losses of R 407C as well as R134a following condensing in a microstructure analysis tunnel were presented. Thermal performance data was performed by means of an analogous heat pipe under the same operational circumstances to demonstrate the benefits of a nano-cylinder over a plain tube. To examine the impact of saturation, point upon that conductivity, practical experiments are conducted across a wide range of input conditions. Again, for fluid layers, correlations against 3 variables from the research were provided. Within the thermal performance prediction model for the immersion method, an appropriate adjustment is again employed for phase equilibrium combination R407C.

Keywords: HFC; Refrigerants; Heat Transfer Coefficient; R407C; R134a; Air conditioners.

INTRODUCTION

Since the late 1960s, furred cylinders have been used to improve condensed heat flow within tube banks in air conditioning units. Once likened to comparable considered a component again under the system parameters, nanofluid pipes exhibit transport properties all through evaporation, which is likely related to a simple increment in efficient interaction and also to the turmoil caused inside the fluid layer by precision blades as well as the surface energy impact on fluid drains [1]. While condensing within nanofluid tubing often occurs at relatively high temperatures, such as in the example with wind capacitors, many empirical numerical simulations described in the literature are

Webology, Volume 18, Number 5, 2021
ISSN: 1735-188X
DOI: 10.29121/WEB/V18I5/25

obtained at normal temperatures because this is more common with moisture coolers [2].

In this paper, the effectiveness of a nanofluid tubing undergoing condensing was systematically investigated at 30°C as well as 60°C. These articles provided personal data derived from directly measuring thermal resistance while compressing R134a and R407C within a 10 mm outside width nanofluid tubing at particle speeds ranging from 120 to 920 kg/(m2 s). This graduated cylinder contains 50 fins with a 0.36 mm fin length as well as a 15° pitch angle and an interior width of 6.12 mm just at the bottom of the grooves. Its wings are triangular in form, with a flat edge as well as a 45° peak inclination [3]. Refrigerants is indeed a single HFC coolant, whereas R407C is a mixture combination of HFC-32, 125, and 134a. R407C has lately been applied to aerosol systems as a brief alternate coolant to R22. R407C was already discovered to cause certain heat conduction issues with the actual usage of vapour equipment, specifically the deterioration of thermophysical properties resulting from mass transport resistive construction [4,5].

Because nanofluid tubing is employed in R407C equipment, it's indeed critical to understand the efficiency of this combination in relation to this specific shape. A comparative friction factor for R22 as well as R407C was tested all in the same nanofluid tubes. Higher condensed degree numerical simulations could be linked to analytical and numerical prediction associations for condensed thermophysical properties. As a result, strong associations may be tested as well as critiqued across a broad range of circumstances, especially in order to comprehensively forecast heat exchange over a wide temperature range [6,7].

EXPERIMENTAL PROCEDURE

The empirical testing was carried out in the Mechanical Engineering Department of Sri Venkateshwara College of Engineering in Tamil Nadu, India. The experiment laboratory is broken down into three circuits: refrigeration, cooled heat, and heating. The coolant is burned up then overheated inside twin pipe heating systems warmed with steam inside the main duct. Therefore, it partly compresses inside the recondense to achieve the desired grade just at the testing segment's intake. Its testing part is a pipe microphone with a coolant condensation process within the inflatable raft against a chilly spillway through the annular.

This measurement heat exchange portion is 400 mm long and is equipped with temperature sensors inserted inside the inner pipe inside the middle of the tube. Multiple thermometers are connected together circularly to form a cross form. High temperatures of nitrogen just at the entrance and exit of a computational domain are monitored utilising isothermal segments as well as heating elements placed in both the refrigeration cycle and or the tubing walls. A magnet connected air compressor may regulate its flow rate separately. To monitor the evaporation both in and out of a petri dish, two dial indicator pressure sensors were linked to manometer tapping.

A centrifugal impact flowmeter installed upstream of a pump measures the coolant volumetric efficiency. An electromagnetic metre measures its chilling flow rate, and just a differentiated multiple metal motive inserted inside mixer compartments measures the temperature increase across an interferometric petri dish. Throughout, mass spectrometry is used to figure out the makeup of a solution moving within the experimental setup. Throughout testing, the average higher cooling rate

Webology, Volume 18, Number 5, 2021
ISSN: 1735-188X
DOI: 10.29121/WEB/V18I5/25

is around 260 l/h, and the absorption thermal gradient stays between 5 and 10 °C. According to a transmission of errors study, the heating was determined to a precision of 5% as well as the heat flux to a precision of 5.5% under normal test settings, with a maximal unknown of 8% under the most extreme situations.

EXPERIMENTAL RESULTS

Figure 1 depicts the condensing cooling rate for R134a as just a proportion of vapour purity at 50 °C cold fluid, expressed also as the porous structure of a simple tube with an inner diameter of eight millimetres. Its heat transfer rate varies as vapour cleanliness increases at a higher peak speed, 900 kg/(m2/s), as found in condensing, which is considered a component. This action of the flippers could clarify the quasi pattern described in Figure 1 at a greater weight speed, about 300 kg/m2/s, that is not found in a straight pipe. Its heat flow is excessive at higher vapour grades whilst decreasing at lower vapour purity, based on the trendline [8]. Figure 1 represents the thermal performance ratio vs. vapour clarity, where another operational effectiveness is described as that of the proportion of the heat flux inside the nanofluid tubes to the heat flux in a comparable diameter smoother tube under similar working circumstances.

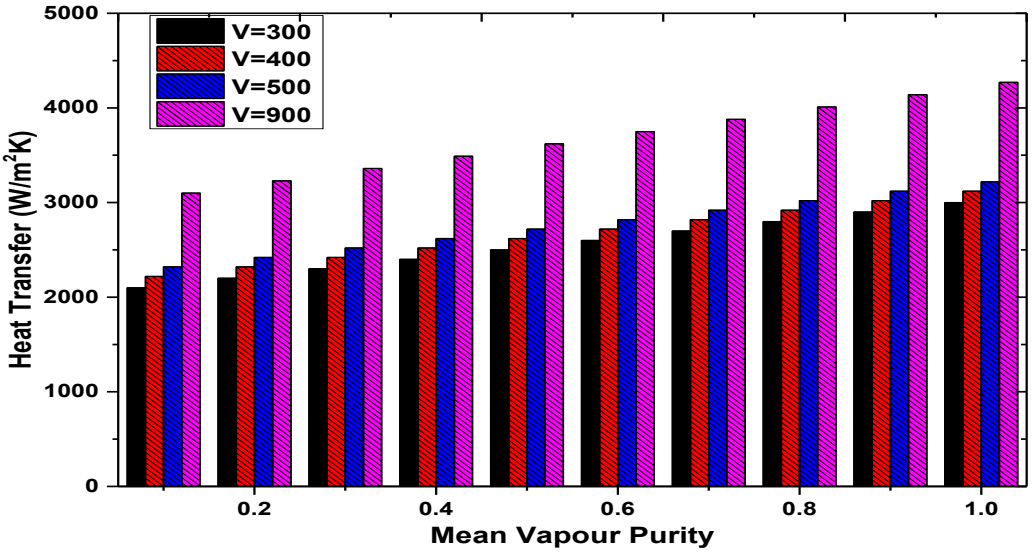

Fig.1. Impact of Heat transfer Rate based on Vapour Conditions and mass velocity

Inside the nanofluid tubes, the inner dimension just at the fin point is utilised as a benchmark. This new iteration estimated heat transfer for a standard plain tube once more. The theory is indeed a semi-analytical connection derived from the best-suited approach using measurements taken by identical researchers in a plain tube with an interior width of 9 mm. The heat removal number is affected by bulk speed as well as condensate reliability; at 50°C melting point, the excitation source's financial strength is attained at 300 kg/(m2 s) weight movement, which could approach 3.2. When the weight acceleration is greater than 300 kg/(m2 s), the efficiency decreases [9,10].

Webology, Volume 18, Number 5, 2021
ISSN: 1735-188X
DOI: 10.29121/WEB/V18I5/25

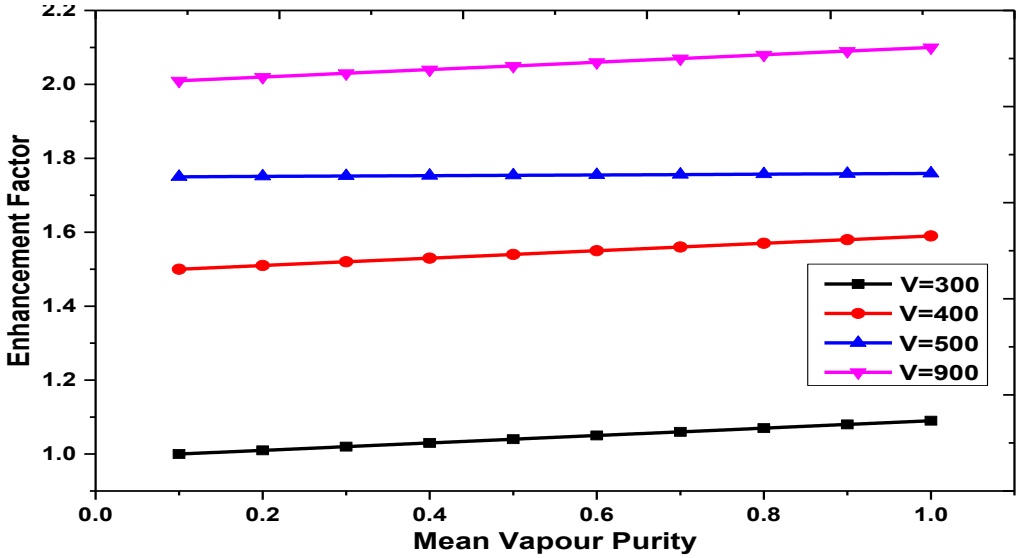

Fig.2. Impact of Enhancement factor based on Vapour conditions and Mass velocity

For 900 kg/m2/s, its dielectric loss is approximately 60% greater compared to the cavity receiver, indicating that thermal efficiency is less than the surface augmentation. The current authors observe the same results when testing with R22.Similarly, its efficiency is lower for G = 150 kg/(m2 s) than for G = 300 kg/(m2 s).This turns out to be an output variable of weight speed in terms of a nanofluid tunnel's ability to transfer heat. This could be because of the airflow inside the tubing. In reality, at high molecular flow rates, deposited thin films might encourage circular flow characteristics, resulting in the highest improvement for just a widely grown motion value.

Figure 2 shows the thermal efficiency determined after condensing of R134a at 60°C operating temperature in the identical nanofluid tubes, whereas Figure 2 shows the thermal conductivity component at the exact latitude. As illustrated in Figures 2 as well as 5, at 300 as well as 900 kg/(m2 s) bulk speed, its value obtained is nearly identical at 50°C as well as 60°C, whereas it differs only 300 kg/(m2 s) as well as higher levels of vapour purity is there a variation in the isotropic source among the hot and cold fluids. To reach a conclusive result just on influence of melting temperature on natural convection at low molar rate and high vapour purity, a greater amount of data obtained at 60°C will be required [11,12].

3.2 Heat transfer coefficients when varying saturation temperature

During the condensing of R134a at a broader range of saturating surface temperatures, the heat flux efficiency with 300 kg/ (m^2s) weight speed is displayed versus time. At 0.8 vapour grade, the surface temperature decreases by 41% from 8000 W/(m^2 K) at 30 °C to 5230 W/(m^2 K) at 70 °C.A lower friction factor equates a smaller pressure change at better adsorption temperatures. Figure 3 depicts the entropy generation forR134a, which isa actually the sum speed at different saturating degrees and equal vapour purity. As predicted, empirically obtained results at 40°C are still greater than data determined at 60°C.

Webology, Volume 18, Number 5, 2021
ISSN: 1735-188X
DOI: 10.29121/WEB/V18I5/25

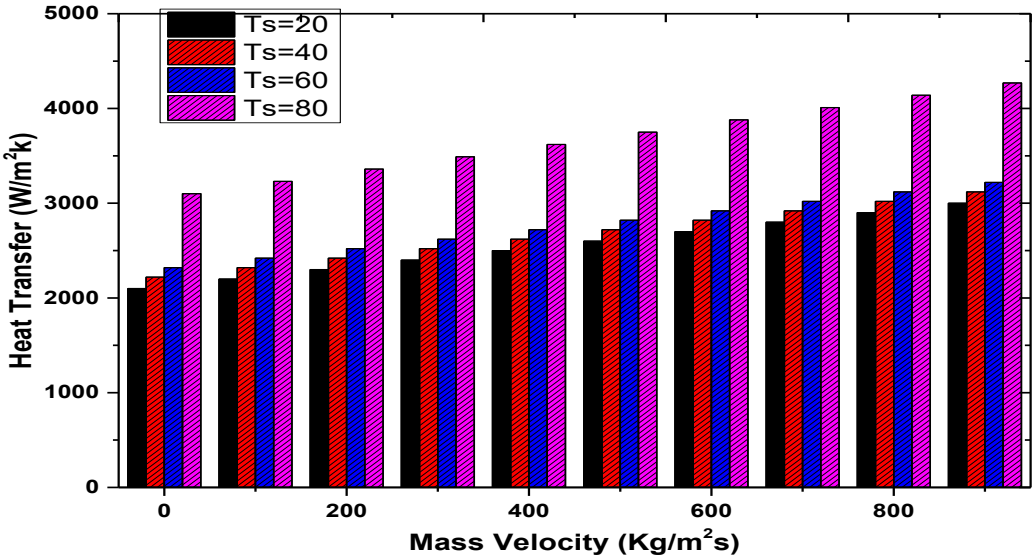

Fig.3. Impact of Heat transfer rate based on the Mass velocity

Though that yields the smallest departure from hard facts at 50°C, it compensates again for the reduction in fluid temperature for better absorption temperatures. This is most likely owing to the information company's limited range of operational heat flux utilised to create the models. Yue and Koyama's association mostly matches empirical temperature profiles at 200 kg/(m2 s), but it also predicts stress-strain curves at higher weight speeds at 50 and 60 °C. In any case, despite the fact that this formula was derived first from the concept of level acceptable, empirical statistics with gravity speeds greater than 400 kg/(m2/s) do not have to fit within the acceptability region [13].

Figure 4 plots empirical and computed estimates of a heat exchanger again for the combination R407C with 0.8 vapour importance due to particle acceleration at 50°C as well as 60°C. All three approaches used for the R134a scenario were likewise employed here now to obtain the thermal coefficient, which is then adjusted using the bells as well as licence adjustment, as previously discussed. In the instance of R134a, a Yu as well as a Managed estimate overestimate the conductivity at 950 kg/m^2 (m^2s). Aside from that, that association does not appear to accurately anticipate the observed pattern for conductivity vs. weight speed. When the models with both the Bells as well as cultural type adjustment are working with a complex at 50°C transition temperature, the concordance improves. That paradigm, like the preceding one, doesn't at all reflect the reduction in parameters associated with ocean warming. At 150 kg/(m^2/s), the theory is used even when the operational circumstances are beyond the researchers' validation limits [14].

Webology, Volume 18, Number 5, 2021
ISSN: 1735-188X
DOI: 10.29121/WEB/V18I5/25

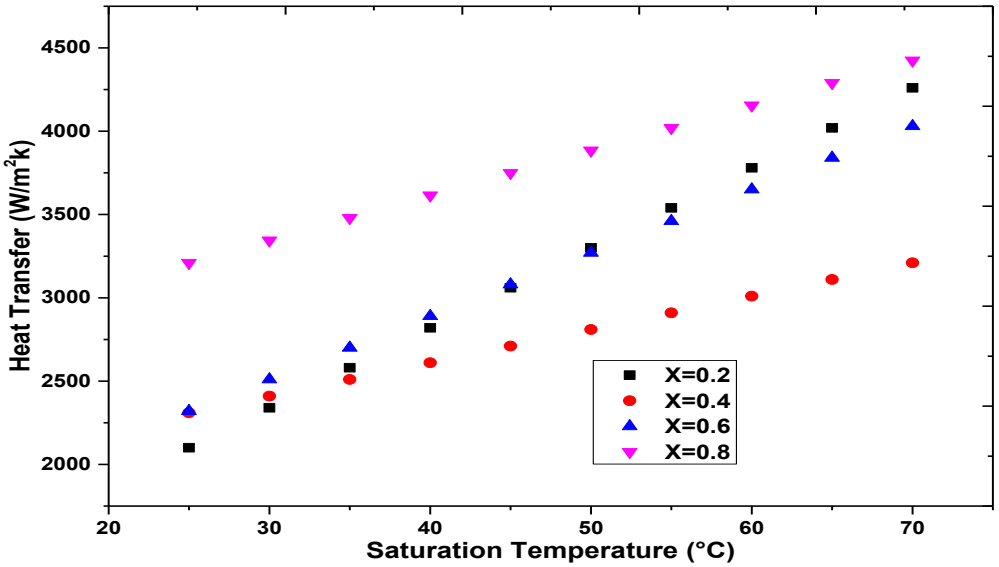

Fig.4. Impact of Heat transfer rate based on the saturation temperature

CONCLUSION

A nanofluid tube was used to conduct in-tube condensate experiments with R134a as well as R407C. Extensive experiments for R134a local heat transmission rates condensed inside nanofluid tubes at 300 kg/ (m^2 s) show that the factor decreases by 41% as pressure drops from 40°C to 60°C.That effect must be considered when building a condensation using nanofluid tubing since the effectiveness of a liquid condensation differs considerably from that of a wind condensation. Investigations of R134a heat flux are indeed illustrated in the form of a straight pipe under operational circumstances. The thermal transfer ratio of R134a is highly dependent on bulk speed inside the tubes, reaching 3.2 for 300 kg/m^2s bulk speed. with a purity of 0.8%.

At higher molecular velocities (900 kg/m2/s), secondary flow is independent of vapour clarity and has a negative price for contact angle improvement. Its mass flow rate during a polymerization reaction significantly influences the transport properties of a combination R407C. Its bulk speed affects both the heat conduction increase caused by the groove as well as the decrease of heat transfer caused by the mixture's phase equilibrium properties. Under identical working circumstances, the thermal conductivity of R407C is smaller compared to R134a within a nanofluid pipe, and this underachievement rises as particle speed drops.

REFERENCES

1. Manjili, F.E.; Yavari, M.A. Performance of a New Two-Stage Multi-Intercooling Transcritical CO 2 Ejector Refrigeration Cycle. Appl. Therm. Eng. 2012, 40, 202–209, doi:10.1016/j.applthermaleng.2012.02.014.
2. Raveendran, P.S.; Sekhar, S.J. Exergy Analysis of a Domestic Refrigerator with Brazed Plate Heat Exchanger as Condenser. J. Therm. Anal. Calorim. 2016, doi:10.1007/s10973-016-5847-2.
3. Hamut, H.S.; Dincer, I.; Naterer, G.F. Exergy Analysis of a TMS (Thermal Management

Webology, Volume 18, Number 5, 2021
ISSN: 1735-188X
DOI: 10.29121/WEB/V18I5/25

System) for Range-Extended EVs (Electric Vehicles). Energy 2012, 46, 117–125, doi:10.1016/j.energy.2011.12.041.

4. Sarkar, J. Performance of Nano Fl Uid-Cooled Shell and Tube Gas Cooler in Transcritical CO 2 Refrigeration Systems. Appl. Therm. Eng. 2011, 31, 2541–2548, doi:10.1016/j.applthermaleng.2011.04.019.
5. Cho, C.; Lee, H.; Won, J.; Lee, M. Measurement and Evaluation of Heating Performance of Heat Pump Systems Using Wasted Heat from Electric Devices for an Electric Bus. 2012, 658–669, doi:10.3390/en5030658.
6. Bhattad, A.; Sarkar, J.; Ghosh, P. Improving the Performance of Refrigeration Systems by Using Nano Fl Uids : A Comprehensive Review. Renew. Sustain. Energy Rev. 2017, 1–14, doi:10.1016/j.rser.2017.10.097.
7. Ahn, J.H.; Kang, H.; Lee, H.S.; Jung, H.W.; Baek, C.; Kim, Y. Heating Performance Characteristics of a Dual Source Heat Pump Using Air and Waste Heat in Electric Vehicles. Appl. Energy 2014, 119, 1–9, doi:10.1016/j.apenergy.2013.12.065.
8. Esen, H.; Esen, M.; Ozsolak, O. Modelling and Experimental Performance Analysis of Solar-Assisted Ground Source Heat Pump System. 2015, 3079, doi:10.1080/0952813X.2015.1056242.
9. Khanmohammadi, S.; Goodarzi, M.; Khanmohammadi, S.; Ganjehsarabi, H. Thermoeconomic Modeling and Multi-Objective Evolutionary-Based Optimization of a Modified Transcritical CO2 Refrigeration Cycle. Therm. Sci. Eng. Prog. 2017, doi:10.1016/j.tsep.2017.10.007.
10. Ma, M.; Yu, J.; Wang, X. Performance Evaluation and Optimal Configuration Analysis of a CO 2 / NH 3 Cascade Refrigeration System with Falling Film Evaporator – Condenser. Energy Convers. Manag. 2014, 79, 224–231, doi:10.1016/j.enconman.2013.12.021.
11. Navarro-esbrí, J.; Molés, F.; Barragán-cervera, Á. Experimental Analysis of the Internal Heat Exchanger in Fl Uence on a Vapour Compression System Performance Working with R1234yf as a Drop-in Replacement for R134a. Appl. Therm. Eng. 2013, 59, 153–161, doi:10.1016/j.applthermaleng.2013.05.028.
12. Goodarzi, M.; Gheibi, A. Performance Analysis of a Modi Fi Ed Trans-Critical CO 2 Refrigeration Cycle. Appl. Therm. Eng. 2015, 75, 1118–1125, doi:10.1016/j.applthermaleng.2014.10.075.
13. Bhattad, A.; Sarkar, J.; Ghosh, P. Energy-Economic Analysis of Plate Evaporator Using Brine-Based Hybrid Nano ° Uids as Secondary Refrigerant. 2018, 26, 1–12, doi:10.1142/S2010132518500037.
14. Jarall, S. Study of Refrigeration System with HFO-1234yf as a Working Fluid ` Me Frigorifique Utilisant Le HFO-1234yf Etude Sur Un Syste Comme Fluide Actif. Int. J. Refrig. 2012, 35, 1668–1677, doi:10.1016/j.ijrefrig.2012.03.007.